Preprint
UCRL-JC-135199

Estimates of Population Inversion for Deep-UV Transitions in Kr-Like Y, Zr, Nb and Mo in a High-Current Reflex Discharge

K.B. Fournier, D. Stutman, V. Soukhanovskii, M. Finkenthal, M.J. May, V.N. Shlyaptsev, W.H. Goldstein

This article was submitted to
44th Annual Meeting of the International Symposium on Optical Science, Engineering, and Instrumentation, Denver, CO, July 18-23, 1999

U.S. Department of Energy

Lawrence
Livermore
National
Laboratory

July 6, 1999

Estimates of population inversion for deep-UV transitions in Kr-like Y, Zr, Nb and Mo in a high-current reflex discharge

K. B. Fournier[a], D. Stutman[b], V. Soukhanovskii[b], M. Finkenthal[b], M. J. May[b], V. N. Shlyaptsev[a] and W. H. Goldstein[a]

[a]Lawrence Livermore National Laboratory, P.O. Box 808 L-41, Livermore, CA 94550
[b]The Johns Hopkins University, Baltimore, MD 21218

ABSTRACT

Kr-like ions are good candidates for FUV lasing since they can be produced in plasmas quite easily. We present results from a spectroscopic investigation of Y IV emission from a high current density, cold cathode reflex discharge. The Y II to Y V emission is recorded in the 200–3000 Å range using photometrically calibrated spectrometers, while the emission of trace aluminum ions serves for plasma diagnostics. The intensities of the Y IV $4d - 5p$ and $5s - 5p$ transitions strongly increase relative to lines from Y II and Y III with increasing plasma current. The spectra studied here are obtained at a current density of 1.75 A/cm^2. Experimental Y IV intensity ratios spanning several excited configurations are compared with collisional radiative predictions of the HULLAC atomic physics package. Good agreement is found for the measured and predicted ratios of 4p^{5}5p to 4p^{5}5s level populations per statistical weight. Finally, the response of the Kr-like system to a fast, transient excitation pulse is examined using the RADEX code. Large transient gains are predicted for several $5s - 5p$ transitions in Y IV, Zr V, Nb VI and Mo VII.

Keywords: Y IV VUV spectra, reflex discharge, transient collisional excitation, gain

1. INTRODUCTION

The emphasis in collisionally pumped short wavelength laser research has recently shifted to development of soft x-ray and XUV lasers created with small scale (low energy) or "table top" drivers.[1] Diado *et al.* have achieved lasing between 6 and 8 nm with Ni-like lanthanide ions from curved slab targets.[2] Rocca *et al.* have made a collisionally pumped transition in Ne-like Ar IX lase at 46.9 nm in a fast capillary discharge.[3,4] It has been observed in saturated operation with a gain coefficient of 1.16 cm^{-1} and a gain-length product greater than 25, achieved with a double pass using iridium mirrors.[4] Lasing media formed with a laser prepulse have demonstrated success with both the Ni-like[5,6] and Ne-like[7] schemes. Transient excitations in plasmas have been proposed as a mechanism for achieving gain-length products orders of magnitude larger than what can be achieved in quasi-steady state (QSS) plasmas[8]; very recently, Dunn *et al.* have demonstrated lasing in Ni-like Pd XIX ions at 14.6 nm excited by transient collisional excitation driven by a modest size 1.1 ps pulse laser.[9]

The current work investigates the kinetics of the energy levels in the Kr-like ions Y IV, Zr V, Nb VI and Mo VII. Earlier work by Klapisch *et al.* [10] has investigated a photopumped lasing transition in Kr-like Mo VII. The Kr-like ion laser has the favorable property that the energy required to excite the lasing level and the energy of the lasing transition are quite similar. This leads to a favorable conversion efficiency for the FUV-EUV transitions of the present work. In our previous work,[11] we showed that modest quasi-steady state gains could be achieved in these ions only at temperatures far in excess of the ions' equilibrium temperatures. It is found that the only way to achieve strong gain in FUV transitions in these Kr-like ions is using a transient excitation pulse.[8,12]

In what follows we present a brief description of the details of models for level kinetics in the Kr-like ion. Then, the spectrum of Y IV as recorded in a high-current reflex discharge with a calibrated spectrometer is shown, and measured ratios of level populations per statistical weight are compared to the observations. Finally, we present calculations for the response of a preformed plasma with mostly Kr-like ions (Y IV, Zr V, Nb VI and Mo VII) to a several ps long excitation pulse. Strong, transient gains are found for several $5s - 5p$ transitions in each ion.

Further author information: Send correspondence to K.B.F.: E-mail: fournier2@llnl.gov

Table 1. Measured transition wavelengths in Å for the lasing transitions of interest to the present work and of the resonant decays which drain the lower level of some of the lasing transitions. A $4p^5$ core has been suppressed in the lasing transitions. Calculated Einstein coefficients for all transitions are listed in sec^{-1}. Numbers in braces represent powers of ten, i.e. X[Y] = $X \times 10^Y$.

	Y IV		Zr V		Nb VI		Mo VII	
	λ^a	$g_u A_{u,l}$	λ^b	$g_u A_{u,l}$	λ^c	$g_u A_{u,l}$	λ^d	$g_u A_{u,l}$
				lasing transitions				
5s 3/2[3/2]$_2$–5p 3/2[1/2]$_1$	2624.3	5.13[+08]	2133.1	8.63[+08]	1796.5	1.26[+09]	1550.5	1.73[+09]
5s 3/2[3/2]$_2$–5p 3/2[3/2]$_2$	2125.5	1.93[+09]	1725.0	2.96[+09]	1451.4	4.11[+09]	1255.2	3.52[+09]
5s 1/2[1/2]$_1$–5p 1/2[1/2]$_0$	2026.1	8.07[+08]	1654.5	5.59[+07]	1400.8	1.27[+09]	1218.1	1.74[+09]
5s 3/2[3/2]$_1$–5p 3/2[1/2]$_0$	2018.8	6.69[+08]	1633.0	1.05[+09]	1375.2	1.31[+09]	1183.3	1.84[+09]
5s 3/2[3/2]$_1$–5p 1/2[1/2]$_0$	1645.1	1.85[+08]	1332.1	3.89[+08]	1121.2	2.01[+08]	964.0	4.10[+08]
4d $^1F_3$–5p 1/2[3/2]$_2$	1345.9	3.82[+09]	841.4	1.11[+10]	589.6	2.15[+10]	441.5[e]	3.93[+10]
4d $^3D_2$–5p 1/2[1/2]$_1$	1308.0	2.26[+09]	822.1	6.70[+09]	577.8	1.34[+10]	434.2[e]	2.35[+10]
4d $^1D_2$–5p 1/2[3/2]$_1$	1306.4	2.26[+09]	823.5	6.61[+09]	579.9	1.31[+10]	436.4[e]	2.33[+10]
4d $^3F_2$–5p 3/2[3/2]$_1$	1275.3	1.91[+09]	809.8	5.45[+09]	572.7	1.08[+10]	432.0[e]	1.88[+10]
				drain transitions				
$4p^6$ ^1S–$4p^5$5s 1/2[1/2]$_1$	370.42	2.69[+10]	292.19	9.75[+10]	238.18	1.69[+10]	198.83	3.57[+10]
$4p^6$ ^1S–$4p^5$5s 3/2[3/2]$_1$	386.82	1.83[+10]	305.24	4.72[+10]	248.73	1.08[+10]	207.78	4.01[+10]

[a] Ref.[15] [b] Ref.[16] [c] Ref.[17] [d] Ref.[18]

[e] J_1l-coupling obtains in the lower level.

2. COLLISIONAL RADIATIVE MODELS FOR KR-LIKE IONS

The ground state of the Kr-like ion is $4s^2 4p^6$; this is a closed shell ground configuration, however, the higher angular momentum d and f orbitals in the n=4 shell are available. This situation is similar to that which obtains in the Pd-like ion laser[13] in which the $4d^{10}$ ground level can undergo Δn=0 excitations to the $4f$ orbital. The J=0 levels of the Kr-like $4p^5 5p$ configuration have strong monopole collisional excitation rates from the $4p^6$ ground configuration. The levels of $4p^5 5p$ are forbidden from E1 (fast) radiative decays to the ground level by parity considerations. Hence, population inversion is achieved in QSS conditions between the $4p^5 5p$ levels and $4p^5 4d$ and $4p^5 5s$ levels, which for levels with J=1, have E1 decays to the ground.

Previous spectroscopic work with the ions in the Kr-like iso-electronic sequence[14] has determined that the levels of the $4p^6$ and $4p^5 4d$ configurations are well described by LS-coupling in Y IV,[15] Zr V[16] and Nb VI.[17] In Mo VII[18] among the levels of the $4p^5 4d$ configuration J_1l-coupling obtains. In every case the levels of the $4p^5 5s$ and $4p^5 5p$ configurations are well described by J_1l-coupling.[15–18] The measured wavelength for the transitions of interest to the present work are listed in Table 1 along with the calculated transition rates. The transition rates in the present work were calculated with the fully relativistic parametric potential code RELAC of Klapisch *et al.* [19,20] Also listed in Table 1 are the wavelengths and transition rates of the resonant "drain" transitions of the lower level for some lasing lines. Details about the calculation of the energy levels and transition rates can be found elsewhere.[11]

The relative populations for the levels of each ion were found in steady state by solving the coupled set of rate equations

$$\frac{dn_j}{dt} = \sum_{i \neq j} n_i R_{i \to j} - n_j \sum_{i \neq j} R_{j \to i} \tag{1}$$

where n_j is the population in level j of a given ion, and $R_{i \to j}$ is the rate at which population leaves level i and goes to some level j, possibly of a neighboring isosequence. Under the QSS approximation,[21–23] dn_j/dt is assumed to be zero for all levels but the ground level of each ion; the level populations in the excited states of each ion then track their respective ground levels. The model for each Kr-like ion includes 301 energy levels generated from configurations with principal quantum number $n \leq 6$. The collisional excitation rates between all levels in the model were computed using RELAC's wave functions in the distorted wave approximation with the program CROSS.[24]

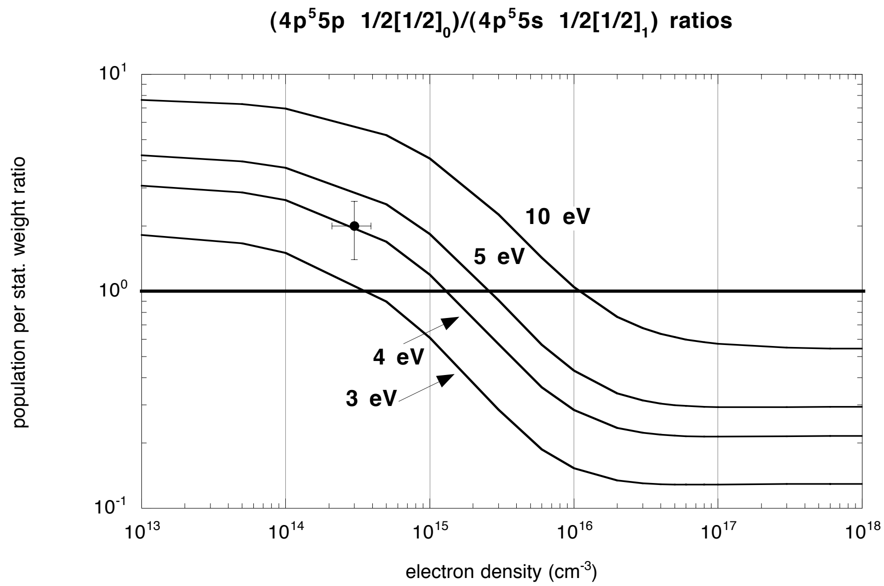

Figure 1. Calculated ratio of Y IV level populations with accounting for plasma self-absorption. Also shown is the experimental value of the ratio of level populations per statistical weight.

The predicted level populations per statistical weight (and the results of our measurements described in section 3) are shown in Figs. 1 to 3. An important difference between the present results and those in our previous work[11] is that the optical thickness of the plasma is accounted for in the escape factor approximation.[25,26] When the predicted curves are above the heavy lines in Figs. 1 to 3, a population inversion exists. If optical depths for the transitions are neglected, the $4p^55p$ over $4p^55s$ population inversion exists out to densities approximately $\times$ 2 higher; optical depth in the $4p^6$ – $4p^54d$ ^1P transition reduces by an order of magnitude the density for which a $4p^55p$ over 4p54d population inversion exists.

Note, the $4p^54d$ ^1P – $4p^55p$ $1/2[1/2]_0$ transition was the focus of our previous work, it had the largest QSS gain of any Kr-like transition. In the present work, it is found not to have an appreciable gain in response to a transient excitation under any conditions. This is due to the relative magnitudes of the $4p^6$ – $4p^54d$ ^1P and $4p^6$ – $4p^55p$ $1/2[1/2]_0$ collisional excitation rates (see section 4). The $4p^55s$ $1/2[1/2]_1$ – $4p^55p$ $1/2[3/2]_2$ and $4p^55s$ $3/2[3/2]_1$ – $4p^55p$ $3/2[3/2]_2$ transitions were reported in our previous work to exhibit QSS gains, they are found not to have any strong response to transient excitation in the present work.

3. EXPERIMENTAL CONFIRMATION OF MODELS

Our collisional-radiative models for the level populations of Y IV have been compared to spectral data from XUV to FUV transitions recorded in a low density, steady state plasma. Y IV spectra are obtained from a cold cathode reflex discharge having metallic Y inserts in Al cathodes (the line emission of Al ions is used for electron temperature and density estimates). The discharge can be continuously operated at current densities up to several A/cm^2 using neon as a buffer gas at pressures of a few mtorr. A schematic drawing of the device is shown in Fig. 4. The discharge parameters are: diameter $\approx$ 0.6 cm, length = 2.5 cm, a current density between 0.5 – 5 A/cm^2 at a 0.5 – 1.5 kV bias voltage and a magnetic field of a few kG. The Y IV emission starts appearing at low current density ($j \approx 1$ A/cm^2); the spectra presented here are obtained at $j \approx 1.75$ A/cm^2. A 0.2 m Minuteman VUV monochromator is used to record spectra in the 300–3000 Å range. The monochromator is equipped with a detector that consists of a scintillator and a photomultiplier tube (PMT). Relative photometric calibration of the monochromator in the 500–2500 Å range was performed in our laboratory using a NIST transfer standard photodiode. The relative efficiency of the monochromator as a function of wavelength is shown in Fig. 5. The wavelength resolution of the monochromator is 0.8–1.5 Å. For line identification, we also utilize a 2 m grazing incidence spectrograph with 0.4–0.7 Å resolution.

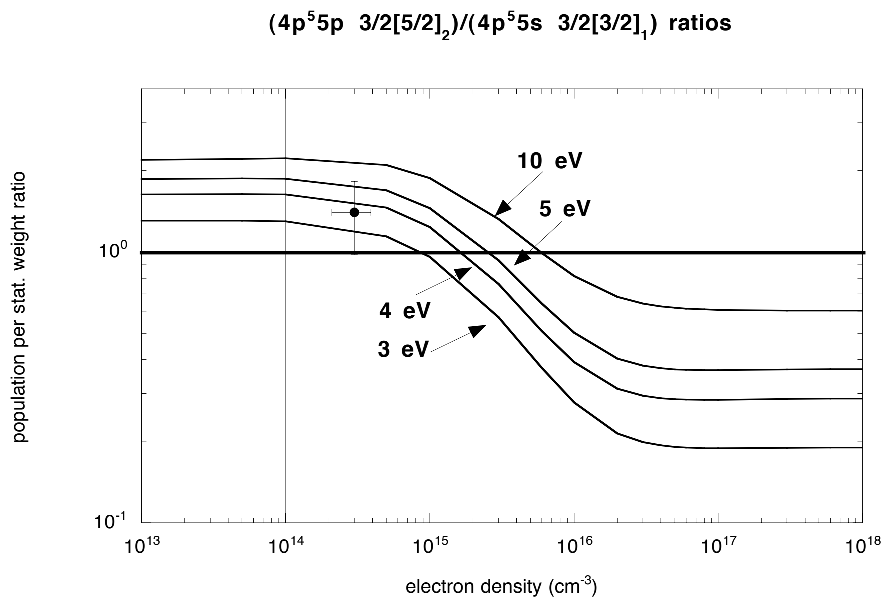

Figure 2. Calculated ratio of Y IV level populations with accounting for plasma self-absorption. Also shown is the experimental value of the ratio of level populations per statistical weight.

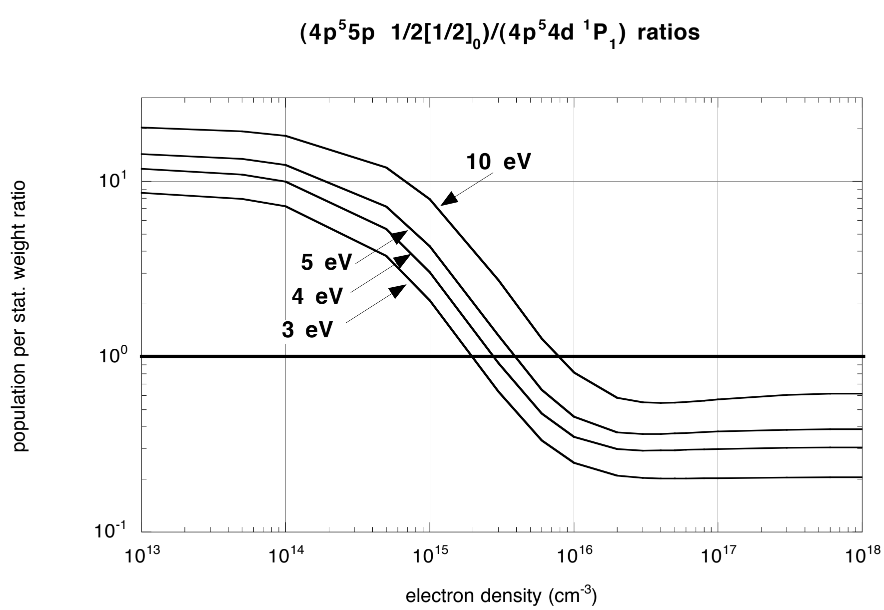

Figure 3. Calculated ratio of Y IV level populations with accounting for plasma self-absorption.

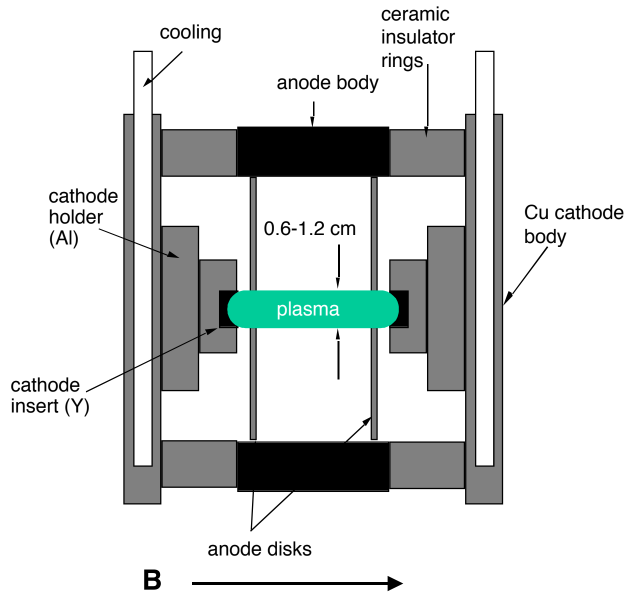

Figure 4. Schematic of the cold cathode reflex discharge at the Johns Hopkins University used to make the observations of the present work.

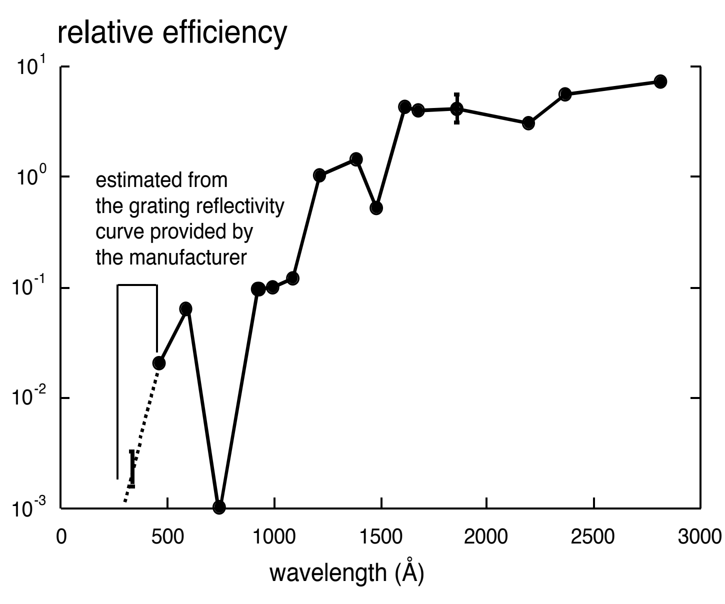

Figure 5. The relative efficiency of the monochromator as a function of wavelength determined by the branching ratio method.

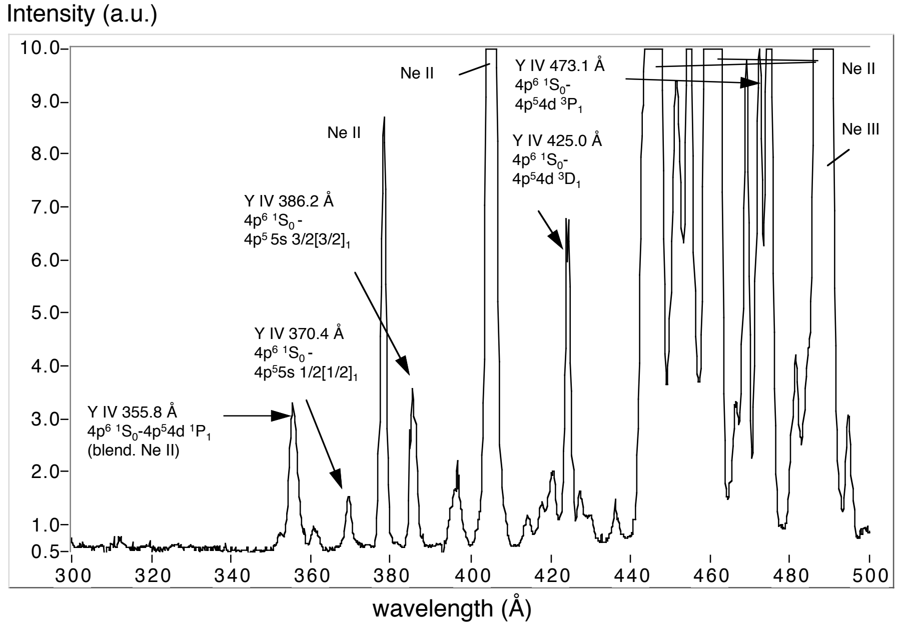

Figure 6. Y IV spectrum in the wavelength range 300 to 500 Å. The $4p-4d$ and $4p-5s$ resonant lines are shown in a spectrum from the cold cathode discharge with neon working gas.

A collisional radiative model using close-coupling atomic data (and taking into account the tail of non-thermal electrons present in reflex discharges[27]) is used to predict the temperature and density dependence of the Al II[28] and Al III[29] spectra. By comparing the predicted and experimental Al intensity ratios, we estimate an electron temperature of 4 to 5 eV and density of a few$\times10^{14}$ cm^{-3} for the region emitting the Y IV lines.

The plasma emission in the spectral range of the $4p-4d$, $4p-5s$, $5s-5p$ and $4d-5p$ transitions in Y IV is presented in Figs. 6, 7, 8 and 9. In the short wavelength region of Fig. 6 the $4p^6\ {}^1S - 4p^54d\ {}^1P$ line at 355.8 Å is slightly blended with Ne II $2p-3d$ lines. The $4p^6 - 4p^54d$ triplet transitions, as well as the $4p^6 - 4p^55s$ lines in Fig. 7 are free of spectral blends. The majority of the strong $4p^55s - 4p^55p$ lines in the 2000 − 2300 Å range shown in Fig. 8 are blended with either Y II[30] or Ne III lines, as are most $4p^55s - 4p^55p$ transitions at longer wavelengths (Fig. 9). For example, the potential $4p^54d - 4p^55p$ J=0 to J=1 laser line at 2610.6 Å is blended with the Ne III $3s'\ {}^3D_3 - 3p'\ {}^3F_4$ transition at 2610.0 Å. However, from the intensity of the nearby $3s'\ {}^3D_3 - 3p'\ {}^3F_{2,3}$ transitions we infer that the Y IV line represents about half of the feature at 2610 Å. The $4p^55s - 4p^55p$ J=0 to J=1 lasing transition at 2026.1 Å is also blended with a Y II line; we observe that in higher current density ($\geq$ 2.5 A/cm^2) discharges the degree of blending is reduced, most of the Y II population is 'burned-through'.

Making allowances for the VUV monochromator calibration uncertainty and for the contribution of line excitation processes other than collisional excitation by Maxwellian electrons, we find reasonable agreement between the experimental Y IV line intensities and those predicted by our collisional radiative model at T_e = 4 eV, $N_e = 10^{14}$ cm^{-3}. In general, for the entire spectral range spanned by Figs. 6 to 9 we find the measured relative intensities of all lines and the predictions of our collisional-radiative model at T_e = 4 eV, $N_e \gtrsim 10^{14}$ cm^{-3} agree to better than ± 30%. Further, using the radiative decay rates in Table 1, we estimate that in the higher current density discharges, population inversion is present in the experimental Y IV spectra. By definition, the intensity of a spectral line is given by

$$I_{\rm u,l} = n_{\rm u} A_{\rm u,l}, \tag{2}$$

where $n_{\rm u}$ is the population in the upper level of the transition. We can find the ratio of population per statistical

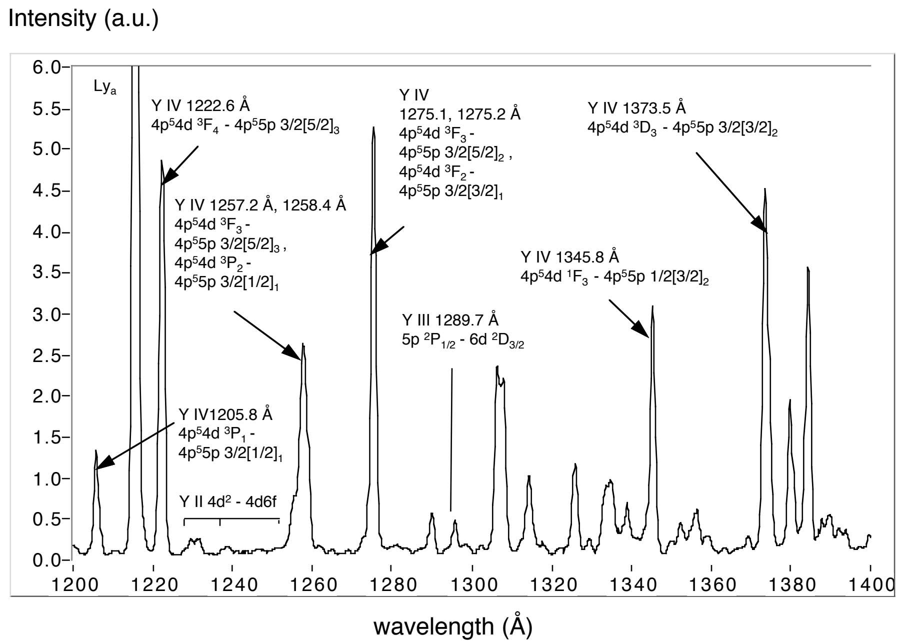

Figure 7. Y IV spectrum in the wavelength range 1200 to 1400 Å. The shorter wavelength $4d - 5p$ transitions are shown in a spectrum from the cold cathode discharge with neon working gas.

weight,

$$\frac{n_{\rm u}/g_{\rm u}}{n_{\rm l}/g_{\rm l}} = \frac{I_{\rm u,l}}{I_{\rm l,f}}\frac{g_{\rm l}A_{\rm l,f}}{g_{\rm u}A_{\rm u,l}}, \tag{3}$$

for levels of interest to the present work. Using the measured intensities of the 4p^{5}5s 1/2[1/2]$_1$ – 4p^{5}5p 1/2[1/2]$_0$ line at 2026.1 Å and the 4p^6 – 4p^{5}5s 1/2[1/2]$_1$ line at 370.4 Å and the calculated transition rates in Table 1, we find an experimental value for the ratio of populations per statistical weight of 2.0. The collisional-radiative model predicts a ratio of 1.9 at a density of 3×10^{14} cm^{-3}. Given the problems of blending and the uncertainty in the calibration of the spectrometer, this is reasonable agreement. Analyzing the 4p^{5}5s 3/2[3/2]$_1$ – 4p^{5}5p 3/2[5/2]$_2$ line at 2491.7 Å and the 4p^6 – 4p^{5}5s 3/2[3/2]$_1$ line at 386.2 Å in the same manner, we find an experimental value for the ratio of populations per statistical weight of 1.4. The collisional-radiative model predicts a ratio of 1.5. In this case there is no problem with blending and the agreement is very good. These results are plotted with the predictions of the collisional-radiative model in Figs. 1 and 2. Due to the relatively low density of Y IV ions in the reflex discharge plasma, the estimated gain coefficient is too small for any significant amplification.

4. GAIN CALCULATIONS FOR RAPID, TRANSIENT HEATING

The above results validate our QSS collisional-radiative models. We now turn our attention to the more promising transient excitation scheme for collisionally pumped soft x-ray lasing. In the transient excitation scheme, population inversion is achieved simply by stronger excitation of the upper lasing level over excitation into the lower level for a temperature jump. The gain is ultimately quenched when levels other than the ground level become significantly populated and begin to excite collisionally the lower lasing level. This is quite different from the QSS picture, where it is the fast radiative decays from the lower level of the lasing transition that enables a population inversion with an upper level that does not have fast radiative decay channels (or whose drain transition is radiatively trapped). This means the 4p^{5}4d ^{1}P – 4p^{5}5p J=0 lasing transition studied in our previous work[11] will not be a candidate for the transient excitation scheme; the 4p^6 ^{1}S – 4p^{5}4d ^{1}P collisional excitation rate will always dominate the 4p^6 ^{1}S –

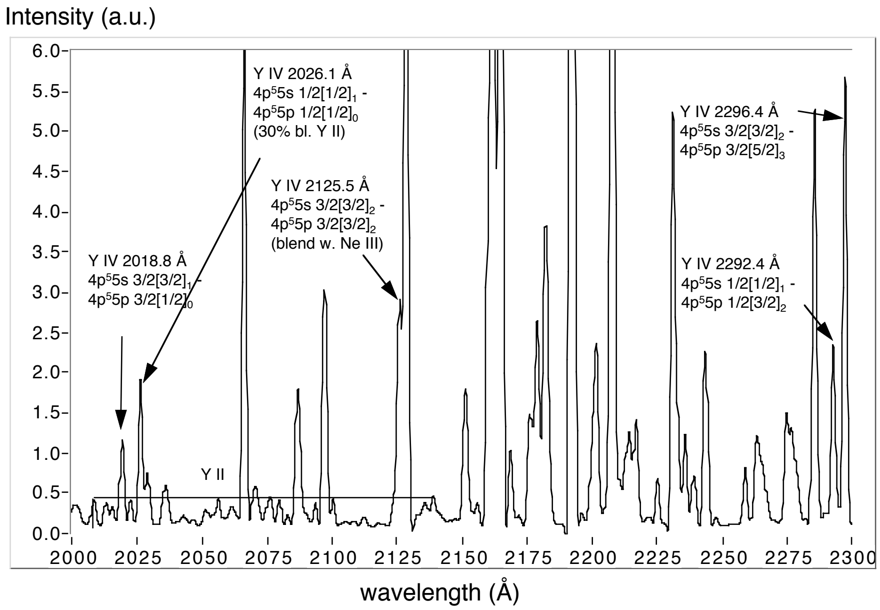

Figure 8. Y IV spectrum in the wavelength range 2000 to 2300 Å. The $5s - 5p$ 'lasing' lines are shown in a spectrum from the cold cathode discharge with neon working gas.

$4p^55p$ J=0 monopole excitation. Only $4d - 5p$ transitions without $4p^54d$ lower levels strongly fed from the ground level will lase. The $4p^6$ ^1S – $4p^55s$ J=1 and $4p^6$ ^1S – $4p^55p$ J=0 transitions have similar excitation energies and the $4p^6$ ^1S – $4p^55p$ J=0 collisional excitation can be dominant over $4p^6$ ^1S – $4p^55s$ J=1. These considerations are reflected in the list of candidate transitions in Table 1.

For transient inversion modeling we have used the RADEX code[8,9] to study the response of the Kr-like transitions in Table 1 to a rapid heating pulse in a moderate density plasma. The initial plasma is assumed to have an electron temperature of 0.05 I_{0z}, where I_{0z} is the ionization potential of ion Z, i.e. 3, 4 and 6.25 eV for the cases of Y IV, Zr V and Mo VII, respectively. This is approximately where the Kr-like ions reach their maximum abundance. The plasma has an electron density of 5×10^{17} cm^{-3} in each case. The plasma for each ion is assumed to be 100 microns thick for purposes of computing the reabsorption in each line transition. The calculations for the Kr-like ions employ the atomic models of our previous work[11]; the Kr-like ion of each element is coupled through valence and inner shell ionization to equally detailed models for the Rb-like and Br-like ions. The initial ion fractions for the three charge states are set to 0.5, 0.5 and 0.0 for Rb-, Kr- and Br-like, respectively, and then are allowed to evolve with the temperature and density conditions. After a time the plasma temperature abruptly jumps to 0.5 I_{0z}, i.e. 30, 40 and 62.5 eV, for Y IV, Zr V and Mo VII, respectively. The plasma stays at this elevated temperature until the predicted gain in the transitions of interest falls off completely.

The resulting gain coefficients for several transitions in each ion are shown in Figs. 10 to 12. The results for Nb VI (not plotted) look very similar to the results for Mo VII (Fig. 12.) The maximum gain coefficients are all $5 < G_{\max} < 70$. These values are generally more than an order of magnitude larger than the maximum QSS gains computed in our previous work.[11] At the time of the temperature jump, the Kr-like ion in each case has a fractional abundance $\gtrsim$ 70%. The abundance continues to increase until the time of peak gain. The gain durations shown here are reasonable for the Kr-like ions at the given conditions. The simplicity of the model (assumed plasma dimensions, step function rise in temperature) means that the estimated gain durations are in no way rigorous. However, we can estimate the maximum gain-length product for these transitions as $GL = G\times c\tau$ where c is the speed of light and τ is the gain duration. For a τ of 70 ps and a maximum gain of 45 (as in Y IV) we find a gain length product $\approx$ 60.

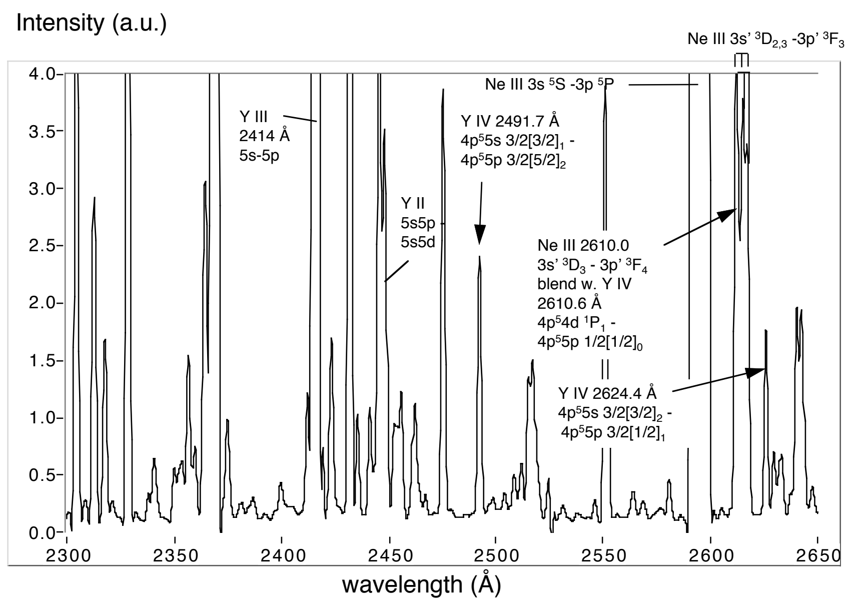

Figure 9. Y IV spectrum in the wavelength range 2300 to 2650 Å. The $4d - 5p$ 'lasing' line is shown in a spectrum from the cold cathode discharge with neon working gas.

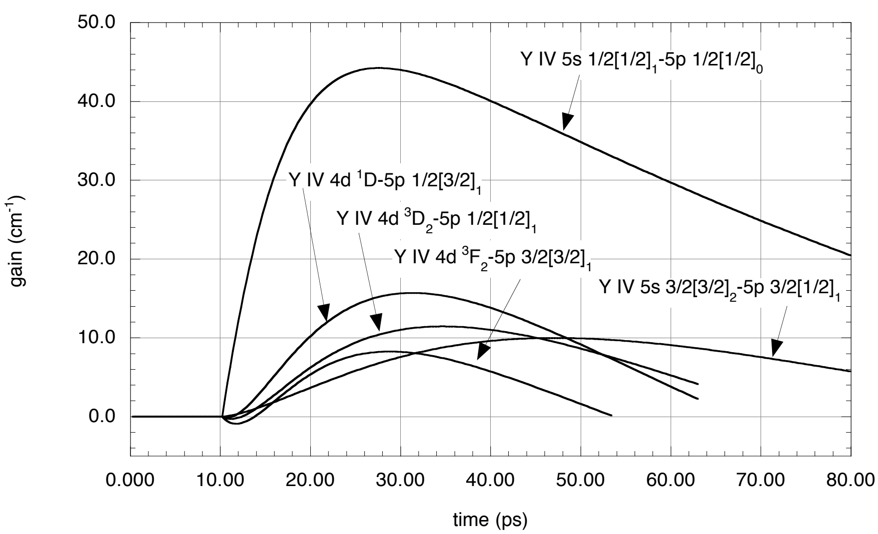

Figure 10. Calculated response of the gain for some $4d - 5p$ and $5s - 5p$ transitions in Y IV to a rapid heating pulse. The plasma is assumed to extend 100 microns with an electron density of 5×10^{17} cm^{-3}.

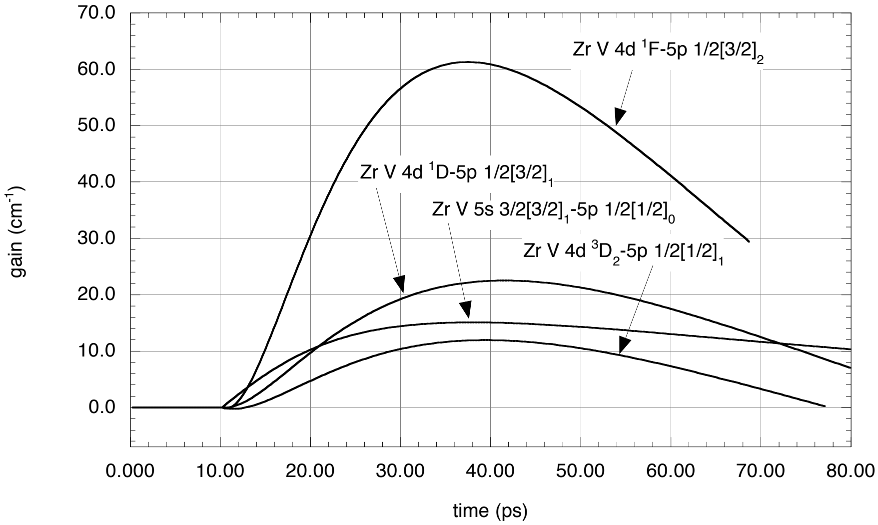

Figure 11. Calculated response of the gain for some $4d - 5p$ and $5s - 5p$ transitions in Zr V to a rapid heating pulse. The plasma is assumed to extend 100 microns with an electron density of $5{\times}10^{17}$ cm^{-3}.

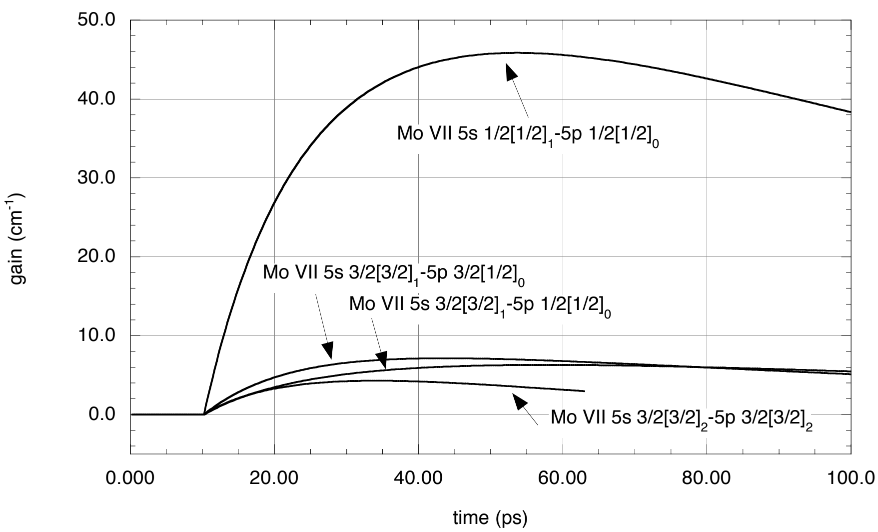

Figure 12. Calculated response of the gain for several $5s - 5p$ transitions in Mo VII to a rapid heating pulse. The plasma is assumed to extend 100 microns with an electron density of $5{\times}10^{17}$ cm^{-3}.

This demonstrates that the Kr-like system has great potential.

It is interesting to note that in all of the elements studied here, transitions with lower lasing levels that do not decay radiatively to the ground state have large transient gains. This situation is usually rare under QSS conditions, with only marginal gains for these transitions, but in the transient case large gains are typical. Examples of such transitions were experimentally obtained recently with substantial (saturated) output.[31] Part (or all) of the $4p^54d$ level structure of the Kr-like ions falls below the $4p^55s$ and $4p^55p$ levels, hence besides inversion between $5p-5s$ levels, they also exhibit inversion between $5p-4d$ levels. However, as stated above, only $4p^54d$ levels not strongly collisionally coupled to the ground level will give rise to transitions with significant gain. For example for Kr-like Zr, the largest gain on any transition occurs on $4p^55p\ 1/2[3/2]_2$ – $4p^54d\ ^1F_3$ (the radiative branching ratio from $4p^55p\ 1/2[3/2]_2$ to $4p^54d\ ^1F_3$ is 0.585). The excitation of the transition's upper lasing level, $4p^6$ – $4p^55p\ 1/2[3/2]_2$ ($1.90[-10]$ cm^{3}s^{-1} at $T_e = 40$eV), this is not largest among excitations to all $4p^55p$ levels. For example, $4p^55p\ 1/2[1/2]_0$ is an order of magnitude more strongly excited from the ground level ($2.39[-09]$ cm^{3}s^{-1} at $T_e = 40$eV), but its strongest radiative decay channel has a branching ratio of 0.697 to the $4p^54d\ ^1P_1$ level. This lower level is populated even more strongly from the ground level, $4p^6$ – $4p^54d\ ^1P_1$ ($2.11[-08]$ cm^{3}s^{-1} at $T_e = 40$eV). Though $4p^54d\ ^1P_1$ decays quickly to the ground level by radiative decay transient gain can not be achieved.

Another similarity the Kr-like ions have with Ne-like ions is the behavior of population inversion as a function of the optical depth of the plasma. In the present work, the transient inversion and gain increased almost 2-3 times when plasma became optically thick. It is found that the major process responsible for the increase is trapping of largest radiative transition $4p^6$ – $4p^54d$. The upper level of this transition then collisionally populates the upper 4p5p levels. Finally, it is observed that several Rb-like transitions exhibit gains comparable to or stronger than those presented here for Kr-like transitions.

5. CONCLUSIONS

We have observed emission from Y II to Y V in the 200–3000 Å range using photometrically calibrated spectrometers. We have used the emission of trace aluminum ions for diagnostics and find the Kr-like Y IV ion emits from a plasma with and electron temperature 4 to 5 eV and an electron density $\approx 10^{14}$ cm^{-3}. The intensities of the Y IV $4d-5p$ and $5s-5p$ transitions increase strongly relative to lines from Y II and Y III with increasing plasma current. Experimental Y IV intensity ratios spanning several excited configurations are compared with quasi-steady state collisional radiative predictions of the HULLAC atomic physics package and agreement to ± 30% is found across the whole spectral range. Further, good agreement is found for the measured and predicted ratios of $4p^55p$ to $4p^55s$ level populations per statistical weight. Optical depths affect the inversions in these configurations only slightly, but nearly totally suppresses inversion in the $4p^55p$ to $4p^54d$ levels. Finally, the response of the Kr-like system to a fast, transient excitation pulse is examined using the RADEX code. Large transient gains are predicted for several $5s-5p$ and $4d-5p$ transitions in Y IV, Zr V, Nb VI and Mo VII. Kr-like ions are good candidates for FUV lasing since they can be produced in plasmas quite easily.

ACKNOWLEDGMENTS

This work was performed under the auspices of the U.S. Department of Energy at the Lawrence Livermore National Laboratory under contract No. W-7405-ENG-48.

REFERENCES

1. S. Basu, P. L. Hagelstein, J. G. Goodberlet, M. H. Muendel, and S. Kaushik *Appl. Phys. B* **57**, p. 303, 1993.
2. H. Daido, Y. Kato, K. Murai, S. Ninomiya, R. Kodama, G. Yuan, Y. Oshikane, M. Takagi, H. Takabe, and F. Koike *Phys. Rev. Lett.* **75**, p. 1074, 1995.
3. J. J. Rocca, V. N. Shlyaptsev, F. G. Tomasel, O. D. Cortázar, D. Hartshorn, and J. Chilla *Phys. Rev. Lett.* **73**, p. 2192, 1994.
4. J. J. Rocca, D. P. Clark, J. L. A. Chilla, and V. N. Shlyaptsev *Phys. Rev. Lett.* **77**, p. 1476, 1996.
5. J. Nilsen, J. C. Moreno, B. J. McGowan, and J. A. Koch *Appl. Phys. B* **57**, p. 309–311, 1993.
6. Y. Li, G. Pretzler, P. Lu, and E. E. Fill *Phys. Rev. A* **53**, p. R652, 1996.
7. Y. Li, G. Pretzler, and E. E. Fill *Phys. Rev. A* **52**, p. R3433, 1995.
8. Y. V. Afanas'ev and V. N. Shlyaptsev *Sov. J. Quantum Electr.* **19**, p. 1606, 1989.

9. J. Dunn, A. L. Osterheld, R. Shepherd, W. E. White, V. N. Shlyaptsev, and R. E. Stewart *Phys. Rev. Lett.* **80**, p. 2825, 1998.
10. M. Klapisch, M. Cohen, W. H. Goldstein, and U. Feldman *Phys. Scripta* **41**, p. 819, 1990.
11. K. B. Fournier, W. H. Goldstein, D. Stutman, M. Finkenthal, V. Soukhanovskii, and M. J. May *Phys. Scripta*, *in press*, 1999.
12. V. N. Shlyaptsev, P. V. Nickles, T. Schlegel, M. P. Kalashnikov, and A. L. Osterheld *Proc. SPIE Int. Soc. Opt. Eng.* **2012**, p. 111, 1993.
13. B. E. Lemoff, G. Y. Yin, C. L. G. III, C. P. J. Barty, and S. E. Harris *Phys. Rev. Lett.* **74**, p. 1574, 1995.
14. J. Reader and G. Epstein *J. Opt. Soc. Am.* **62**, p. 273, 1972.
15. G. Epstein and J. Reader *J. Opt. Soc. Am.* **72**, p. 476, 1982.
16. J. Reader and N. Acquista *J. Opt. Soc. Am.* **69**, p. 239, 1979.
17. J. Ekberg and J. Reader *J. Opt. Soc. Am. B* **11**, p. 415, 1994.
18. J. Reader and U. Feldman *J. Opt. Soc. Am. B* **7**, p. 253, 1990.
19. M. Klapisch *Computer Phys. Comm.* **2**, p. 239, 1971.
20. M. Klapisch, J. Schwob, B. Fraenkel, and J. Oreg *J. Opt. Soc. Am.* **67**, p. 148, 1977.
21. D. Bates, A. Kingston, and R. McWhirter *Proc. Royal Soc. (London) A* **267**, p. 297, 1962.
22. D. Bates, A. Kingston, and R. McWhirter *Proc. Royal Soc. (London) A* **270**, p. 155, 1962.
23. V. Boiko, I. Skobelev, and A. Faenov *Sov. J. Plasma Phys.* **10**, p. 82, 1984.
24. A. Bar-Shalom, M. Klapisch, and J. Oreg *Phys. Rev. A* **38**, p. 1773, 1988.
25. T. Holstein *Phys. Rev.* **72**, p. 1212, 1947.
26. E. E. Fill *J. Quant. Spectrosc. Radiat. Transfer* **39**, p. 489, 1988.
27. D. Stutman, M. Finkenthal, A. K. Bhatia, J. L. Schwob, S. P. Regan, M. J. May, and H. W. Moos, "The effect of non-maxwellian electrons, charge exchange and Penning processes on the XUV emission of Y ions from a reflex discharge plasma," in *Proceedings of the 10th International Colloquium on UV and X-ray Spectroscopy of Astrophysical and Laboratory Plasmas*, E. Silver and S. Kahn, eds., p. 169, Cambridge University Press, (Berkeley, CA), 1992.
28. M. Finkenthal, A. Littman, D. Stutman, S. Kovnovich, P. Mandelbaum, J. L. Schwob, and A. K. Bhatia *Phys. Scripta* **41**, p. 502, 1990.
29. M. Finkenthal, A. Littman, D. Stutman, and A. K. Bhatia *J. Phys. B: At. Mol. Phys.* **22**, p. L115, 1989.
30. A. E. Nilsson, S. Johansson, and R. L. Kurucz *Phys. Scripta* **44**, p. 226, 1991.
31. M. P. Kalachnikov, P. V. Nickles, M. Schnürer, W. Sandner, V. N. Shlyaptsev, C. Danson, D. Neely, E. Wolfrum, J. Zhang, A. Behjat, A. Demir, G. J. Tallents, P. J. Warwick, and C. L. S. Lewis *Phys. Rev. A* **57**, p. 4778, 1998.